

See discussions, stats, and author profiles for this publication at: <https://www.researchgate.net/publication/231651361>

# Mechanisms of Size Reduction of Colloidal Silver and Gold Nanoparticles Irradiated by Nd:YAG Laser

ARTICLE *in* THE JOURNAL OF PHYSICAL CHEMISTRY C · MAY 2009

Impact Factor: 4.77 · DOI: 10.1021/jp808300q

---

CITATIONS

54

READS

96

## 3 AUTHORS, INCLUDING:



Alexander Pyatenko

National Institute of Advanced Industrial S...

36 PUBLICATIONS 884 CITATIONS

[SEE PROFILE](#)

# Mechanisms of Size Reduction of Colloidal Silver and Gold Nanoparticles Irradiated by Nd:YAG Laser

Alexander Pyatenko,\* Munehiro Yamaguchi, and Masaaki Suzuki

Research Institute of Genome-based Biofactory, National Institute of Advanced Industrial Science and Technology (AIST), Sapporo 062-8517, Japan

Received: September 18, 2008; Revised Manuscript Received: April 8, 2009

We consider two possible mechanisms for silver and gold particle size reduction by laser irradiation and demonstrate that electron ejection can practically be neglected for all possible parameters of a nanosecond Nd:YAG laser, used without beam focusing. We evaluate the applicability of this process for different experimental conditions and conclude that more intensive lasers must be used in order for electron ejection to play an important role. We also provide direct experimental evidence for the validity of the particle heating–melting–evaporation mechanism for experiments conducted with an Nd:YAG laser.

## 1. Introduction

Silver and gold nanoparticles of different sizes and shapes have been attracting much attention due to their unusual size- and shape-depending properties.<sup>1–4</sup> Lasers are used more and more often for fabrication,<sup>5–9</sup> size reduction,<sup>10–16</sup> and reshaping<sup>13,17</sup> of these particles. Size reduction of nanoparticles after laser irradiation is a well-known phenomenon.<sup>10–13</sup> Different mechanisms of size reduction have been proposed by different research groups: Kamat and co-workers<sup>10</sup> concluded from their picosecond photoabsorption spectroscopic measurements that the photoejection of electrons from a particle into a solution caused ionization and Coulomb explosion of the ionized particle. Takami et al.<sup>11</sup> studied the fragmentation of gold nanoparticles by nanosecond laser pulses and proposed a simple explanation for their size reduction through the heating–melting–evaporation mechanism. To confirm this model, Takami et al. measured the temperature of gold nanoparticles by measuring the emission spectra of gold particles with a photon counter system and found that 0.2  $\mu$ s after the laser pulse the particle temperature was  $2500 \pm 100$  K, which is much higher than the gold melting temperature,  $T_m$  (Au) = 1337 K.<sup>11</sup> Recently, Mafune and co-workers<sup>18</sup> detected photoelectrons ejected from gold nanoparticles irradiated by nanosecond laser pulses and, thereby, seemed to confirm the mechanism proposed by Kamat et al.<sup>10</sup> for nanosecond lasers. In our previous work,<sup>17</sup> we have used the particle heating–melting–evaporation model to calculate “soft” laser irradiation, which, in turn, was used for silver nanoparticles synthesis. The well controllable size of particles synthesized and narrow particle size distribution provide good evidence of the validity of this model.

Although the primary act of laser beam interaction with a particle is the absorption of the laser’s photons by the particle’s electrons, the subsequent process can develop then in two different ways. Electrons can rapidly accumulate sufficient energy to leave the particle. Alternatively, the energy of electrons will rapidly transfer to the crystal lattice due to the good “heat transfer” between the electrons and phonons, with further particle melting and evaporation.

In this paper we identify the experimental parameters responsible for both scenarios and estimate the ranges of these parameters corresponding to each mechanism.

## 2. The System Studied

In this paper, we consider the system composed of mono-disperse spherical silver or gold nanoparticles suspended in pure water. Particle sizes can be varied from 10 to 100 nm. Colloids are irradiated by one of three main wavelengths of an Nd:YAG laser: the fundamental ( $\lambda = 1064$  nm), second harmonic ( $\lambda = 532$  nm), or third harmonic ( $\lambda = 355$  nm). Pulse duration,  $\tau_0$ , is adopted as equal to 10 ns, and laser beam diameter,  $D_0$ , equals 7 mm. Both values are very typical for Nd:YAG lasers. Maximum pulse energy,  $(A_0)_{\max}$ , was adopted equal to 1 J/pulse for the fundamental wavelength, 0.5 J/pulse for the second harmonic, and 0.3 J/pulse for the third harmonic. Those values correspond to the following maximum values of laser energy flow density (or laser intensity),  $I_0$ :  $2.6 \times 10^{12}$  W/m<sup>2</sup> (fundamental wavelength),  $1.3 \times 10^{12}$  W/m<sup>2</sup> (second harmonic), and  $7.8 \times 10^{11}$  W/m<sup>2</sup> (third harmonic), where

$$I_0 = \frac{A_0}{\tau_0 S_0} = \frac{4A_0}{\pi \tau_0 D_0^2} \quad (1)$$

All results of this paper can be applied for different colloid systems consisting of the same particles suspended in other liquids. For that, it is necessary to know how the absorption of a laser beam by a particle depends on the particle’s surrounding media.

## 3. Theoretical Study of Electron Ejection

**3.1. Multophoton Excitation.** First, we have to estimate the possibility of multiphoton excitation in our system. For numerical estimations we can use the multiphoton parameter introduced in<sup>19</sup>

$$X = (eE_0k_F)/m_e\omega^2 \quad (2)$$

Here,  $e$  and  $m_e$  are the electron charge and mass,  $E_0$  is the amplitude of electric field in laser plane wave, and  $k_F$  is the radius of Fermi sphere for free electron gas in a metal particle

\* Corresponding author, alexander.pyatenko@aist.go.jp.

$$k_F = (2m_e E_F)^{1/2}/\hbar \quad (3)$$

where  $E_F$  is Fermi energy of the free electron gas in a metal particle

$$E_F = \hbar^2/2m_e(3\pi^2 N_e/V_p)^{2/3} \quad (4)$$

For silver and gold, each atom has only one conductive electron. Therefore, in these metals, the number of conductive electrons in the particle,  $N_e$ , is equal to the number of atoms in this particle,  $N_a$ . Both metals have an face-center cubic (fcc) crystal structure, with a similar lattice constant:  $a_{Au} \approx a_{Ag} = 0.408$  nm.<sup>20</sup> Thus, the number of atoms per spherical particle with diameter  $d_p$  and volume  $V_p = d\pi_p^3/6$ , will be

$$N_e = N_a = \frac{2\pi}{3} \left( \frac{d_p}{a} \right)^3 \quad (5)$$

In such a case, the Fermi energy and Fermi radius will be constant values:  $E_F = 24.1\hbar^2/(2m_e a^2) = 8.87 \times 10^{-19}$  J = 5.54 eV, and  $k_F = 4.91/a = 1.2 \times 10^8$  cm<sup>-1</sup>.

By using the known relations between energy flow density,  $I_0$ , and amplitudes of electric and magnetic fields in a plane wave

$$I_0 = E_0 H_0 = E_0^2 \sqrt{\frac{\epsilon_0}{\mu_0}} \quad (6)$$

where  $\epsilon_0$  and  $\mu_0$  are the permittivity and permeability of vacuum, we will obtain

$$X = \frac{4.91}{a} \frac{e}{m_e} \left( \frac{\mu_0}{\epsilon_0} \right)^{1/4} \frac{\sqrt{I_0}}{\omega^2} \quad (7)$$

or

$$(I_0)_{cr} = \frac{a^2(X)_{cr}^2 m_e^2}{24.1} \left( \frac{\epsilon_0}{\mu_0} \right)^{1/2} \omega^4 \quad (7a)$$

Assuming that multiphoton processes become essential when  $X$  exceeds 1, the following critical values of laser intensities,  $(I_0)_{cr}$ , were calculated:  $6 \times 10^{15}$  W/m<sup>2</sup> (for the fundamental wavelength,  $\lambda = 1064$  nm),  $9 \times 10^{16}$  W/m<sup>2</sup> (for the second harmonic,  $\lambda = 532$  nm), and  $5 \times 10^{17}$  W/m<sup>2</sup> (for the third harmonic,  $\lambda = 355$  nm). These values are several orders of magnitude higher than the maximum possible values of Nd:YAG laser intensities calculated above. We can thus conclude that the multiphoton processes can be neglected when Nd:YAG laser is used without beam focusing.

Another criterion for multiphoton excitation can be obtained by comparing the photon density in a laser beam

$$n_{ph} = \frac{I_0}{\hbar\omega c} \quad (8)$$

with the density of free (conductive) electrons in a metal particle

$$n_e = \frac{N_e}{v_p} = \frac{4}{a^3} \quad (9)$$

The new parameter, therefore, will be equal to

$$Y = \frac{n_{ph}}{n_e} = \frac{a^3 I_0}{4\hbar c \omega} \quad (10)$$

or

$$(I_0)_{cr} = \frac{4\hbar c}{a^3} Y_{cr} \omega \quad (10a)$$

Assuming that the critical value of this new parameter is also equal to 1, we calculated the critical values of laser intensities,  $(I_0)_{cr}$ , needed to for multiphoton processes and obtained  $3 \times 10^{17}$  W/m<sup>2</sup> for  $\lambda = 1064$  nm,  $7 \times 10^{17}$  W/m<sup>2</sup> for  $\lambda = 532$  nm, and  $1 \times 10^{18}$  W/m<sup>2</sup> for  $\lambda = 355$  nm. All three values are much higher than the maximum possible values of Nd:YAG laser intensities. The estimation made with the maximum possible values of Nd:YAG laser intensities demonstrated that the photon density in a laser beam was at least 6–7 orders lower than the density of free electrons in metal particles.

**3.2. Photoelectric Process.** Two processes for ejection of electrons from a metal into a vacuum are known: the photoelectric effect and thermionic emission.

A hot electron can be ejected from a particle when it absorbs a laser photon with energy  $\hbar\omega$ , if the electron thermal energy,  $\epsilon$ , exceeds  $E_F + W - \hbar\omega$ , where  $W$  is a work function of metal ( $W_{Ag} = 4.26$  eV,  $W_{Au} = 5.1$  eV,<sup>21</sup> photon energy equals to 1.17, 2.33, and 3.51 eV for fundamental, second, and third harmonic, respectively). This mechanism can occur through the intraband (Drude) absorption or interband transition. As demonstrated in ref 22 for gold nanoparticles irradiated by 351 nm light, the second (interband) process is negligible compared to the first one. This result can be transferred to silver particles, because the interband gap for silver exceeds that for gold.<sup>23</sup> Of course, it does not mean that interband absorption does not take place in our system, but it cannot contribute significantly in the direct photoelectric process. Therefore, we can consider that the photoelectric process can occur through the intraband absorption alone for all parameters considered in this paper.

As it was shown in ref 22 for small gold nanoparticles irradiated by 351 nm light, the relative amount of photoelectrons is negligibly small compared to thermoelectrons. The reason for such low efficiency of the photoelectric process is the relatively low concentration of highly excited electrons that can be ejected by the photoeffect. Our evaluation results in Supporting Information demonstrate that for the experimental conditions used in ref 22 (a gold particle with a diameter 5.2 nm irradiated by a 351 nm laser beam), the relative amount of hot electrons that can be ejected from the particle by absorbing a laser photon is 0.2%. When the laser wavelength increases to 532 nm, the fraction of such hot electrons increases to 0.3–0.4%, mainly due to the increase in electron temperature. When gold was replaced with silver, the work function decreased from 5.1 to 4.26 eV, and therefore it is possible to expect that the relative role of the photoeffect can increase. As will be demonstrated in the Supporting Information, the maximum possible fraction of hot electrons that can be ejected from the particle by absorbing laser photons increases from 0.2% for gold to 1.4% for silver. Thus, the fraction of electrons suitable for direct photoejection can increase by several times when gold is replaced by silver. Taking into account that the total amount of photoelectrons for gold particle was <1% of the thermoelectrons,<sup>22</sup> we can expect that the situation will not change dramatically in the case of silver, and for both cases we conclude that the role of the photoelectric process is negligible and that the main photoejection process is thermionic emission.

**3.3. Thermionic Emission.** The efficiency of thermionic emission is defined by electron temperature.

The process of heating the whole system can be divided into two steps: fast heating of the electrons and slow heating of particle crystal lattice. For the first process we will apply the

two-temperature model that has been extensively used in the literature to describe such systems.<sup>24–28</sup> The governing equations are

$$\begin{aligned} c_e \frac{dT_e}{dt} &= -\frac{G}{v_p}(T_e - T_p) + \frac{L}{v_p} \\ c_p \frac{dT_p}{dt} &= \frac{G}{v_p}(T_e - T_p) - \frac{S}{v_p} \end{aligned} \quad (11)$$

where  $T_e$  and  $T_p$  are the temperatures of the electrons and the phonons,  $c_e$  and  $c_p$  are the heat capacities of the electrons and the phonons,  $v_p$  is the particle volume,  $L$  is the laser power absorbed by conductive electrons of the particle through the plasmon absorption mechanism per unit time,  $G$  is the electron–phonon coupling constant, and  $S$  is the particle heat loss per unit time. It is assumed here that the electron gas (conductive electrons) is distributed homogeneously throughout a particle's volume. It is also assumed that  $T_e$  and  $T_p$  are constant throughout the particle's volume, (i.e., they do not depend on spatial coordinates). Two equations of system 11 can be combined into one equation for the temperature difference between  $T_e$  and  $T_p$

$$\frac{d(\Delta T)}{dt} = -a\Delta T + b \quad (12)$$

where

$$a = \frac{G}{v_p} \left( \frac{1}{c_e} + \frac{1}{c_p} \right)$$

and

$$b = \frac{1}{v_p} \left( \frac{L}{c_e} + \frac{S}{c_p} \right)$$

The electron heat capacity,  $c_e = \gamma T_e$ , where  $\gamma = 63 \text{ J}/(\text{m}^3 \text{ K}^2)$ , is much smaller than that of the lattice,  $c_e \ll c_p$ , for all temperatures considered here. As indicated in ref 17, heat loss is negligible compared with laser energy absorbed by a particle in time periods shorter than the pulse duration. Thus, we have

$$a = \frac{G}{v_p c_e} = \frac{G}{v_p \gamma T_e}$$

and

$$b = \frac{L}{v_p c_e} = \frac{L}{v_p \gamma T_e}$$

Because  $c_e$  depends on the electrons temperature,  $c_e = T \gamma_e$ , the coefficients in eq 12 are variables. Taking into account that for initial period  $T_p \ll T_e$ , and thus,  $T_e \approx \Delta T$ , we have

$$a = \frac{G}{v_p \gamma T_e} = \frac{a^*}{\Delta T}$$

$$b = \frac{L}{v_p \gamma T_e} = \frac{b^*}{\Delta T}$$

where  $a^*$  and  $b^*$  are already constant, and eq 12 is transformed to

$$\frac{d(\Delta T)}{dt} = -a^* + \frac{b^*}{\Delta T} \quad (12a)$$

This equation has the analytical solution

$$\ln \left( 1 - \frac{a^*}{b^*} \Delta T \right) + \frac{a^*}{b^*} \cdot \Delta T = -\frac{a^{*2}}{b^*} \quad (13)$$

It describes the near exponential growth of  $\Delta T$  to its maximum value

$$\Delta T_{\max} = \frac{b^*}{a^*} = \frac{L}{G}$$

The laser power absorbed by a particle per unit time (shorter than the pulse duration) is

$$L = I_0 \sigma_{\text{abs}}^\lambda(d_p) \quad (14)$$

where  $I_0$  is the laser intensity defined by eq 1 and  $\sigma_{\text{abs}}^\lambda(d_p)$  is the particle absorption cross section (dependent on  $\lambda$ ). The last values can be calculated by classical Mie theory<sup>1,29</sup> for particles of different sizes. The electron–phonon coupling constant,  $g$ , where  $G = g v_p$ , can be found in literature for different metals. We adopted the following experimental values from refs 27, 28, and 30:  $g_{\text{Ag}} = (3.5 \pm 0.5) \times 10^{16} \text{ W}/(\text{K m}^3)$  and  $g_{\text{Au}} = (3.0 \pm 0.5) \times 10^{16} \text{ W}/(\text{K m}^3)$ . Finally, for the first process of intensive electron heating we have

$$\Delta T_{\max} = \frac{3 I_0 \text{eff}_{\text{abs}}^\lambda(d_p)}{2 g d_p} \quad (15)$$

where

$$\text{eff}_{\text{abs}}^\lambda(d_p) = \frac{4 \sigma_{\text{abs}}^\lambda(d_p)}{\pi d_p^2} \quad (16)$$

is the absorption efficiency—a dimensionless ratio of the absorption cross section to the particle cross section. The values of absorption efficiency, calculated by Mie theory,<sup>1,29</sup> are shown in Figure 1 as functions of particle diameter for the fundamental, second, and third harmonic wavelengths of an Nd:YAG laser.

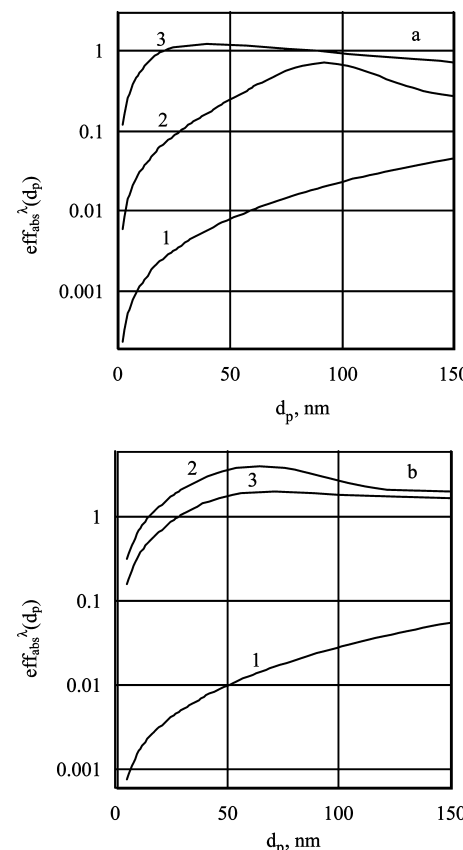


**Figure 1.** Absorption efficiency of spherical silver (a) and gold (b) nanoparticles,  $\text{eff}_{\text{abs}}^\lambda$ , as a function of particle diameter,  $d_p$ , calculated by classical Mie theory<sup>7</sup> for fundamental,  $\lambda = 1064 \text{ nm}$  (1), second,  $\lambda = 532 \text{ nm}$  (2), and third,  $\lambda = 355 \text{ nm}$  (3), harmonic wavelengths of an Nd:YAG laser.

This dependence of absorption efficiency on particle diameter and laser wavelength will appear in all results below.

The characteristic time of this process is

$$t_0 = \frac{b^*}{a^{*2}} = \frac{L v_p \gamma}{G^2} = \frac{6 \gamma I_0 \sigma_{\text{abs}}^\lambda}{\pi g^2 d_p^3} \quad (17)$$

Introducing the absorption efficiency as above, we obtain

$$t_0 = \frac{6 \gamma}{4 g^2 I_0} \frac{\text{eff}_{\text{abs}}^\lambda}{d_p}$$

and remembering that  $\Delta T_{\text{max}} = L/G$ , we find that

$$t_0 = \frac{\gamma}{g} \Delta T_{\text{max}} \quad (17a)$$

Therefore, the characteristic time of this process is defined completely by the  $\Delta T_{\text{max}}$  value.

For example, for  $\Delta T_{\text{max}} = 100$  K,  $t_0 = 0.2$  ps, and for  $\Delta T_{\text{max}} = 1000$  K,  $t_0 = 2$  ps. These values of characteristic time correspond well with the electron–phonon coupling times, measured by El-Sayed et al.<sup>31,32</sup>

After this period of intensive electron heating, the relatively slow heating of the crystal lattice becomes the dominant process. In this period electron temperature continues to increase slowly to keep the temperature difference,  $\Delta T$ , constant.

The maximum possible lattice temperature is restricted by the melting point. After melting, however, the liquid particle can be heated to the boiling point,  $T_b(\text{Ag}) = 2485$  K,  $T_b(\text{Au}) = 3200$  K.<sup>33</sup> To estimate the electrons' maximum possible temperature, we assumed that once the particle melts the heat transfer between electrons and the liquid particle would remain the same as the e–p coupling between electrons and the crystal lattice before melting. With such an assumption, the electrons' maximum possible temperature could be estimated as

$$(T_e)_{\text{max}} = T_b + \Delta T_{\text{max}} \quad (18)$$

where  $\Delta T_{\text{max}}$  is defined by eq 15. Such estimated maximum possible electron temperature following  $\Delta T_{\text{max}}$  depends on the  $I_0$  value and, thus, will be different for different laser intensities. If we use the maximum possible laser intensities for each of the three main wavelengths of an Nd:YAG laser, as adopted in section 2, we obtain the maximum temperatures of the electron gas that can be reached by using the different wavelengths of an Nd:YAG laser. These maximum electron temperatures are plotted in Figure 2 as functions of particle diameter for both silver and gold particles. As indicated in this figure, the maximum temperature to which electron gas can be heated by a Nd:YAG laser strongly depends on the particle diameter and laser wavelength, as well as on particle material (gold or silver).

The analytical solution (15) for  $\Delta T_{\text{max}}$  was obtained assuming that the electron–phonon coupling,  $g$ , does not depend on temperature. As demonstrated in the literature,<sup>22,34</sup> however, when the electron temperature becomes rather high, the temperature dependence of electron–phonon coupling can take place. For silver this effect becomes noticeable when the electron temperature exceeds 5000 K.<sup>34</sup> As can be seen in Figure 2a, the maximum possible electron temperature for all silver nanoparticles remains below 5000 K for all possible parameters of an Nd:YAG laser. Thus, the approach that assumes constant electron–phonon coupling and provides the analytical solution is applicable for silver nanoparticles irradiated by a Nd:YAG laser. For gold the temperature dependence of electron–phonon coupling becomes noticeable after 3000 K<sup>34</sup> or 4000 K.<sup>22</sup> However, we can expect that the correction in maximum

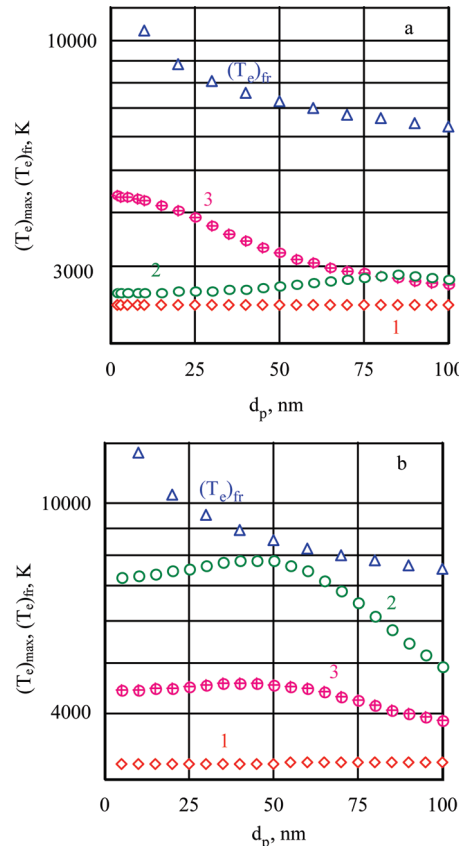


**Figure 2.** Maximum temperatures of electron gas in silver (a) and gold (b) nanoparticles of different diameters that can be reached by irradiating these particles with fundamental,  $\lambda = 1064$  nm (1), second,  $\lambda = 532$  nm (2), and third,  $\lambda = 355$  nm (3), harmonic wavelengths of an Nd:YAG laser. Maximum pulse energies were adopted equal to 1 J/pulse (1), 0.5 J/pulse (2), and 0.3 J/pulse (3). The fragmentation temperatures,  $(T_e)_{\text{fr}}$ , are depicted for comparison.

electron temperature will not be essential and that we can use the same approach for gold nanoparticles, considering that the analytical solution (15) was obtained for the initial process of particle interaction with a laser beam, when mainly the electrons were heated and when, therefore, the electron temperature,  $T_e$ , was very close to temperature difference,  $\Delta T$ . Let us also note that this correction can only decrease the maximum electron temperature: it cannot increase it. These upper limits of electron temperature permit us to estimate the possibilities of thermoelectric emission.

An electron can be ejected by the thermionic effect if the electron thermal energy,  $\varepsilon$ , exceeds  $E_F + W$ . Such electrons have sufficient energy to escape from the metal. The fraction of electrons with energy exceeding  $\varepsilon$ , can be calculated for each temperature from the equation

$$\frac{n_\varepsilon}{N}(T) = \int_{\varepsilon}^{\infty} f_e \sqrt{e} de / \int_0^{\infty} f_e \sqrt{e} de \quad (19)$$

where  $f_e = 1/(1 + \exp[e - \mu]/kT)$  is the Fermi–Dirac distribution function, and  $e^{1/2}$  comes from the density of states around  $e$ . Fermi energy,  $E_F$ , defined by eq 4, can be used instead of chemical potential,  $\mu$ , because the system considered here is well below the Fermi temperature,  $T_F = E_F/k$ , which in our case equals  $6.4 \times 10^4$  K.

The critical fraction of ejected electrons, which leads to particle fission, can be estimated by using the “liquid drop model”.<sup>35,36</sup> In this model, developed for small gaseous clusters

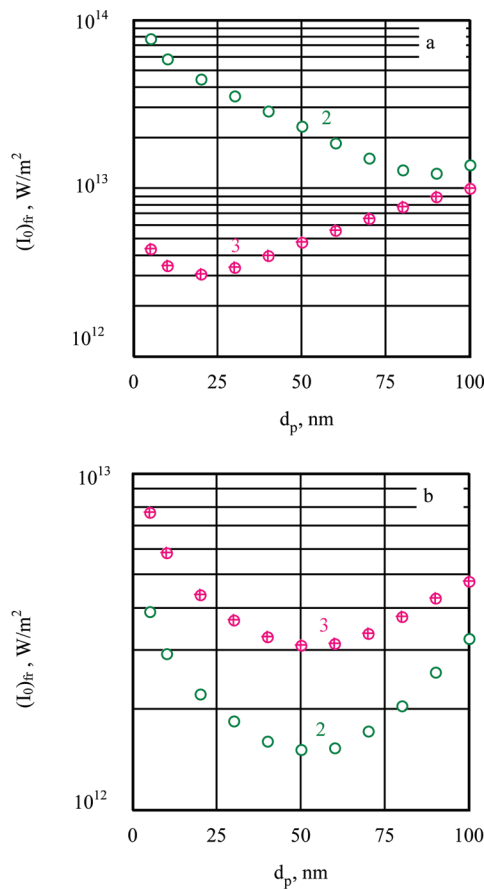


**Figure 3.** Minimum laser intensities needed to heat the electron gas in silver (a) and gold (b) nanoparticles of different diameters up to fragmentation temperature,  $(T_e)_r$ . Calculations were made for fundamental,  $\lambda = 1064$  nm (1), second,  $\lambda = 532$  nm (2), and third,  $\lambda = 355$  nm (3), harmonic wavelengths of an Nd:YAG laser.

of different metals, the cluster fission process is treated as competition between Coulomb and surface forces. For nanoparticle fragmentation, this model was adopted by Mafune and co-workers.<sup>18</sup> The probability of cluster fissility depends on the value of parameter X

$$X = \left( \frac{q^2}{n} \right) / \left( \frac{16\pi r_{ws}^3 \sigma_s}{e^2} \right) = \left( \frac{q^2}{n} \right) / \left( \frac{q^2}{n} \right)_{cr} \quad (20)$$

where  $q$  is the number of charges per cluster,  $n$  is the number of atoms in this cluster,  $r_{ws}$  is the Wigner–Seitz radius of this cluster, and  $\sigma_s$  is the surface tension. Index cr means the critical value of the  $(q^2/n)$  ratio. When  $(q^2/n) = (q^2/n)_{cr}$ ,  $X = 1$ , the cluster is expected to decay instantaneously (Rayleigh limit). Fission is expected to start when  $X \approx 0.3$ . Using the critical values,  $(q^2/n)_{cr}$ , equal to 0.91 and 1.11 for silver and gold, respectively,<sup>35</sup> and adopting  $X = 0.3$ , we calculate the  $(q^2/n)$  and then the  $(q/n)$  ratios for silver and gold nanoparticles of different sizes. Applying to our system, particle charge,  $q$ , equals the number of electrons ejected from the particle,  $n_e^{ej}$ ,  $n$  equals  $N_a = N_e$ , defined by formula 5, and calculated  $(q/n)$  ratios just equals the minimum fractions of electrons ejected from a particle that cause the particle fragmentation,  $(n_e^{ej}/N_e)_{fr}$ .

Therefore, by performing the numeric integration in eq 19, we calculate the fraction number of electrons that can be thermally ejected from the particle for different electron temperatures, and then by comparing this fraction number with the minimum fraction number that causes the particle fragmentation, we calculate the minimum electron temperature,  $(T_e)_{fr}$ ,

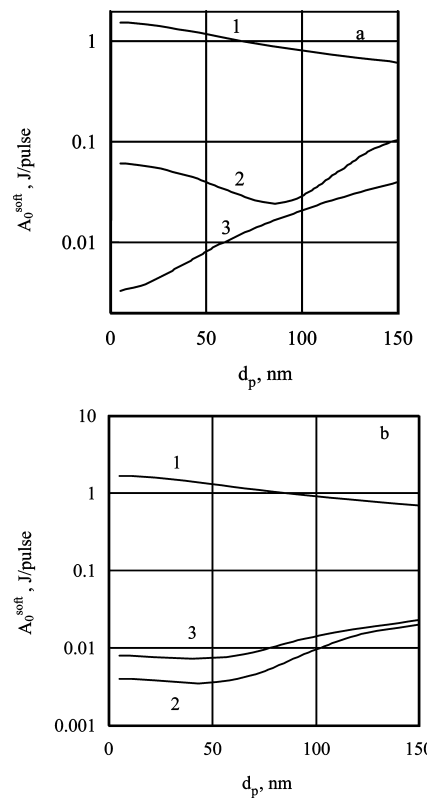


**Figure 4.** Minimum pulse energy,  $A_0^{\text{soft}}$ , needed to initiate the process of evaporation of silver (a) and gold (b) particles of different diameters. Calculations were made for fundamental,  $\lambda = 1064$  nm (1), second,  $\lambda = 532$  nm (2), and third,  $\lambda = 355$  nm (3), harmonic wavelengths of an Nd:YAG laser.

at which the fragmentation process can start. These fragmentation temperatures,  $(T_e)_{fr}$ , calculated for silver and gold particles of different sizes are depicted in Figure 2 for comparison with the maximum electron temperatures that can be achieved with an Nd:YAG laser. To estimate the accuracy of our calculations, we made the same calculations for  $X = 0.2$  and  $0.4$  (according to ref 36 all experimental data for the fission of clusters of different metals correspond well to this range of parameter X). The relative error in fragmentation temperature is rather small and increases from about 2% to 3% when particle size decreases from 100 to 10 nm.

It can be seen from the figure that in the case of silver the difference between  $(T_e)_{max}$  and  $(T_e)_{fr}$  is too large for the total range of particle diameters and laser wavelengths. Even taking into account the precision of our estimation, we can conclude that in silver nanoparticles irradiated by Nd:YAG laser the electrons cannot be heated enough to cause the particle photofragmentation. The same things can be said of gold nanoparticles irradiated by fundamental ( $\lambda = 1064$  nm) or third harmonic ( $\lambda = 355$  nm) wavelengths of an Nd:YAG laser. In this case the maximum electron temperatures are also well below the fragmentation temperatures. A similar situation can be observed when we irradiate rather small ( $d_p \leq 25$  nm) or rather large ( $d_p \geq 75$  nm) gold particles with the second harmonic wavelength ( $\lambda = 532$  nm). The situation looks different when middle size gold particles are irradiated by the second harmonic. In this case the fragmentation temperature,  $(T_e)_{fr}$ , exceeds the maximum possible electron temperature,  $(T_e)_{max}$ , of 700 K. Taking into account the precision of both temperature estimation processes, we can conclude that for these midsize gold particles ( $d_p \approx 40$ –70 nm), the photofragmentation process caused by thermionic electron ejection can be started, when these particles

were irradiated by the second harmonic ( $\lambda = 532$  nm) with laser pulse energy close to 0.5 J/pulse. Mafune et al.<sup>18</sup> detected photoelectrons ejected from small gold nanoparticles ( $d_p = 8 \pm 5$  nm) irradiated by the third harmonic of an Nd:YAG laser. Our calculations show that for such experimental conditions the maximum electron temperature ( $(T_e)_{\max} \approx 4500$  K) must be much lower than the fragmentation temperature ( $(T_e)_{\text{fr}} \approx 13000$  K). To observe the photofragmentation process, the authors<sup>18</sup> had to use a highly focused laser beam. Beam focusing increases the laser intensity and then, according to eq 15, raises electron temperature. However, beam focusing creates different electron temperatures in different particles along the beam, which makes interpreting experimental results more difficult. According to our estimations, the easiest way to observe the photopragmentation for an Nd:YAG laser is to irradiate gold particles with diameters of about 50 nm by the second harmonic ( $\lambda = 532$  nm). In such experiments, defocusing or slightly focusing the laser beam with maximum possible pulse energy can be used.

Finally, we calculate the minimum laser intensity needed to initiate particle fragmentation,  $(I_0)_{\text{fr}}$ , i.e., the laser intensity that heats the particle's conductive electrons just up to fragmentation temperature,  $(T_e)_{\text{fr}}$ . The results are shown in Figure 3 for gold and silver particles of different diameters irradiated by second ( $\lambda = 532$  nm) and third ( $\lambda = 355$  nm) harmonics of an Nd:YAG laser. Similar to the  $(T_e)_{\max}$  value, the critical laser intensity depends strongly on particle size and laser wavelength. These strong dependences result from the fact that  $(I_0)_{\text{fr}}$  is a function of the particle absorption efficiency, which in turn strongly depends on  $d_p$  and  $\lambda$  (see Figure 1). For silver nanoparticles, the smallest  $(I_0)_{\text{fr}}$  values can be obtained by using the third harmonic ( $\lambda = 355$  nm). In such a case for all ranges of particle diameters ( $d_p = 10$  to 100 nm), the critical value of laser intensity needed to initiate Coulomb fragmentation will be  $(I_0)_{\text{fr}}(\lambda = 355) \geq 10^{13} \text{ W/m}^2$ . That is 1 order of magnitude larger than the maximum possible laser intensity available for the third harmonic. For the second harmonic, ( $\lambda = 532$  nm), the critical value of laser intensity will increase 1 order,  $(I_0)_{\text{fr}}(\lambda = 532) \geq 10^{14} \text{ W/m}^2$ , and for the fundamental wavelength ( $\lambda = 1064$  nm), it will increase 1 order more. For gold nanoparticles, the smallest  $(I_0)_{\text{fr}}$  values can be obtained by using the second harmonic ( $\lambda = 532$  nm). In such a case, for the entire range of particle diameters ( $d_p = 10$  to 100 nm), the critical value of laser intensity needed to initiate Coulomb fragmentation will be  $(I_0)_{\text{fr}}(\lambda = 532) \geq 4 \times 10^{12} \text{ W/m}^2$ . By using particles with diameters of about 50 nm, it is possible to reach the Coulomb fragmentation condition with a laser intensity of about  $1.5 \times 10^{12} \text{ W/m}^2$ , which is rather close to the maximum possible value. In all other cases  $(I_0)_{\text{fr}}$  values are essentially larger than the maximum possible values. Thus, we can conclude that for practically all possible parameters of an Nd:YAG laser, the possibility of particle fragmentation caused by electron ejection is very small. We can also conclude that the process of photofragmentation caused by electron ejection will not be effective if the laser intensity is less than  $10^{12} \text{ W/m}^2$ .

#### 4. Experimental Study of Particle Evaporation

As indicated above, the characteristic time of the intensive electron heating process is on the order of picoseconds. Because the pulse duration is 10 ns, the period of slow particle heating is 3 to 4 orders of magnitude higher. Due to this tremendous difference between the two characteristic times of these two processes, particle melting and evaporation can occur at laser intensities much less than the minimum laser intensities needed for particle photofragmentation caused by Coulomb forces. For

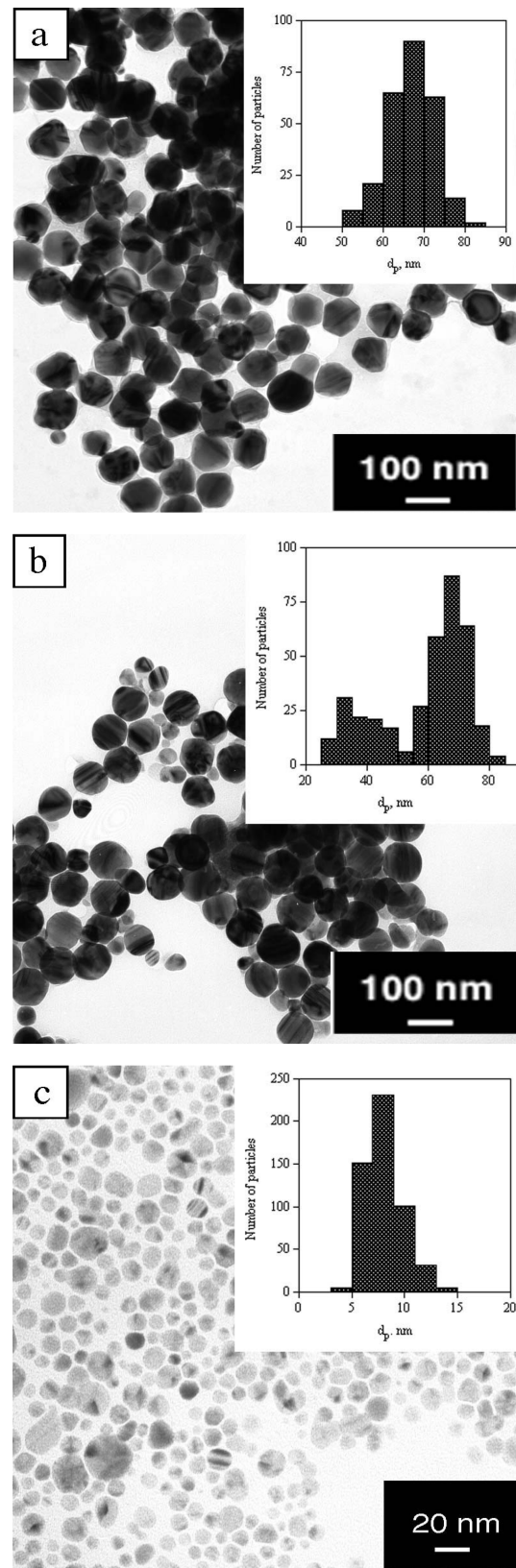


**Figure 5.** TEM photographs and PSD histograms made for silver colloid with initial particle size of  $68.7 \pm 6.3$  nm, irradiated with three different laser powers: 0.015 J/pulse (a), 0.030 J/pulse (b), and 0.28 J/pulse (c).  $\lambda = 532$  nm.

example, according to our calculation, a laser beam composed of the third harmonic ( $\lambda = 355$  nm) and pulse energy  $A_0 = 0.03$  J/pulse can completely evaporate silver nanoparticles with diameters of 40 nm or less. Furthermore,  $\Delta T_{\max}$  values calculated

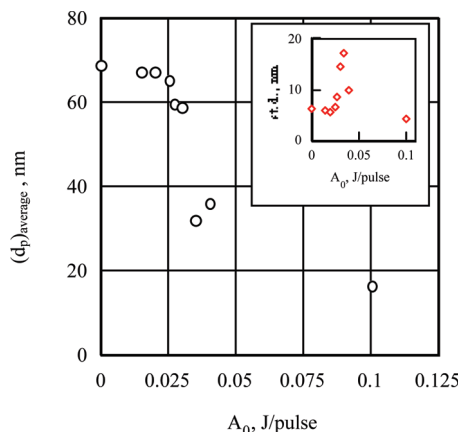


**Figure 6.** Average size of silver particles in colloid, with initial particle size of  $68.7 \pm 6.3$  nm, irradiated with different laser pulse energies. Second harmonic of an Nd:YAG laser ( $\lambda = 532$  nm) was used. Insert shows how the standard deviation in average particle size changed with laser pulse energy.

from eq 15 were 100–200 K, which is 1 order of magnitude smaller than the values needed for Coulomb fragmentation. As another example, irradiation of gold nanoparticles with diameters of 80 nm or less by a laser beam composed of the second harmonic ( $\lambda = 532$  nm) and  $A_0 = 0.03$  J/pulse fully evaporates these particles. At the same time,  $\Delta T_{\max}$  values were about 200–300 K, which is also too small for the electron ejection process.

Thus, if sufficient laser beam energy is absorbed by a particle, the particle can melt and evaporate. Experimental evidence of particle melting was obtained earlier.<sup>11,17</sup> It would be very attractive to have experimental proof of the particle evaporation process. To achieve that, it is generally necessary to calculate the amount of absorbed energy responsible for particle evaporation from energy balance and then to calculate what part of particle volume will be evaporated by this energy. On the other hand, experimentally it is possible to find how much the particles are reduced in size after irradiation. For such measurements, a colloid of monodisperse particles is needed. Another problem is that, as reported in our previous paper,<sup>16</sup> the partial particle vaporization can be accompanied by some other particle growth. This secondary particle growth process can essentially change the particle size distribution. Because the intensity of the secondary particle growth increases with increasing intensity of evaporation, we have to work under conditions close to the threshold of evaporation to avoid these problems. This particle evaporation threshold or the minimum laser pulse energy,  $A_0^{\text{soft}}$ , needed to initiate the process of particle evaporation can be calculated by using the thermodynamic approach:

$$Q_{\text{abs}}^{\text{soft}}(d_p) = \frac{A_0^{\text{soft}}}{S_0} \sigma_{\text{abs}} \lambda = \rho_p \frac{\pi d_p^3}{6} [c_p^s(T_m - T_0) + \Delta H_m + c_p^l(T_b - T_m)] \quad (21)$$

Following our previous paper,<sup>17</sup> we used index “soft” for this evaporation threshold condition, comparing it with “hard” irradiation that causes full evaporation of a particle.<sup>16</sup> All physical and thermodynamic constants used in eq 1, i.e., silver density,  $\rho_p$ , heat capacities,  $c_p^s$  for solid and  $c_p^l$  for liquid, and melting heat,  $\Delta H_m$ , were adopted from Perry.<sup>33</sup> This minimum laser pulse energy, needed to initiate the process of particle evaporation,  $A_0^{\text{soft}}$ , is plotted in Figure 4 as a function of particle diameter for fundamental, second, and third harmonic wavelengths of an Nd:YAG laser. This information could be very

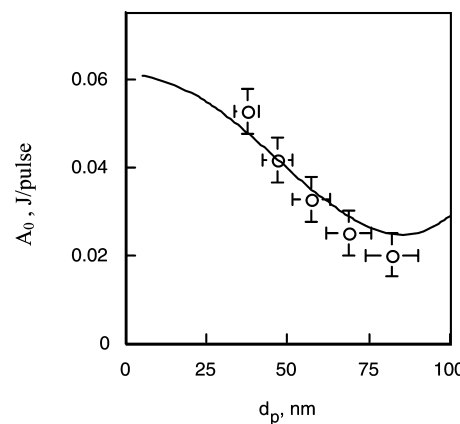


**Figure 7.** Experimental points  $A_0(d_p)$  and theoretical curve  $A_0^{\text{soft}}(d_p)$  for the minimum laser pulse energy needed to initiate the process of silver nanoparticle evaporation. Laser wavelength is 532 nm.

useful for researchers who want to use laser irradiation for particle reshaping. All calculations can be made for one individual laser pulse because, as it was shown above, the particle will cool down completely in the period between two consecutive pulses.

On the other hand, the particle evaporation threshold can be determined experimentally for different particle sizes. We measure the condition for initiating particle evaporation with five different colloids containing monodisperse silver nanoparticles with different average diameters ( $37 \pm 3.2$  nm,  $46 \pm 5.0$  nm,  $53.8 \pm 6.7$  nm,  $68.7 \pm 6.3$  nm, and  $82.3 \pm 7.6$  nm), prepared using our original method.<sup>17</sup> Small amounts (5 mL) of each colloid were irradiated by the second harmonic of an Nd:YAG laser ( $\lambda = 532$  nm) with different laser powers for 1 h. After each irradiation experiment, samples were prepared for transmission electron microscopy (TEM) analysis by placing one droplet of colloid onto a microgrid. A Hitachi H-800 model (voltage = 200 kV) was employed for TEM observation. Five or more microphotographs of different areas of the mesh were used to measure the particle size distribution (PSD). Over 200 particles were counted to plot a histogram and measure the PSD. The results of PSD measurements made for one colloid with an initial particle size of  $68.7 \pm 6.3$  nm are shown in Figure 5 for three different laser powers. It was observed that when the laser pulse energy was 0.015 J, the average particle size remained the same, indicating that the particle evaporation process had not yet started for such laser pulse energy. For  $A_0 = 0.030$  J/pulse, the PSD exhibited two peaks, demonstrating that many particles smaller than the initial particles had already appeared in the colloid. Therefore, the particle had already started to evaporate. For  $A_0 = 0.28$  J/pulse the process of particle evaporation was completed. Only small particles existed in the colloid. The average size of the particles ( $(d_p)_{\text{av}} = 8.0 \pm 1.8$  nm) is practically the same as reported in our previous works<sup>16,17</sup> for the similar conditions.

The dependence of average particle diameter on laser pulse energy,  $d_p(A_0)$  measured for a colloid with an initial particle size of  $68.7 \pm 6.3$  nm is presented in Figure 6. As can be seen from this figure, the average particle size decreases rapidly after evaporation starts, and the standard deviation of this average size increases rapidly due to the bimodal PSD and decreased rapidly with further increase of laser pulse energy. After analyzing the  $d_p(A_0)$  dependences measured for all five colloids, we estimated the threshold laser power values, i.e., the  $A_0(d_p)$  values, at which evaporation begins for different particle sizes. The results are depicted in Figure

7, where experimentally found threshold values,  $A_{0i}(d_{pi})$ , are plotted together with theoretical curve,  $A_0^{\text{soft}}(d_p)$ , calculated as described above. Good agreement between experimental results and the theoretical curve demonstrates that the particle heating–melting–evaporation mechanism<sup>11,16,17</sup> works well under the considered experimental conditions.

## 5. Conclusion

On the basis of our theoretical estimations and experimental results, we can conclude that different mechanisms of particle size reduction apply under different experimental conditions. The probability of the processes caused by electron ejection depends on the laser energy flow density  $I_0$ , which, in turn, is a function of particle diameter and laser wavelength. If  $I_0$  is less than  $10^{12} \text{ W/m}^2$ , the particle heating–melting–evaporation mechanism is solely responsible for reducing the particle size. We believe that the results presented here will be useful to all specialists using lasers in particle size controlling, resizing, and reshaping.

**Supporting Information Available:** Calculated fractions of hot electrons that can be ejected from particles by the direct photoelectric effect made for maximum possible temperatures of electron gas, which in turn, is a function of particle diameter and laser wavelength. This material is available free of charge via the Internet at <http://pubs.acs.org>.

## References and Notes

- (1) Kreibig, U.; Vollmer, M. *Optical Properties of Metal Clusters*; Springer Series in Material Science 25; Springer: Berlin, 1995.
- (2) Kamat, P. V. *J. Phys. Chem. B* **2002**, *106*, 7729.
- (3) Kelly, L.; Coronado, E.; Zhao, L.; Schatz, G. C. *J. Phys. Chem. B* **2003**, *107*, 668.
- (4) Noguez, C. *J. Phys. Chem. C* **2007**, *111*, 3806.
- (5) Mafune, F.; Kohno, J.; Takeda, Y.; Kondow, T.; Sawabe, H. *J. Phys. Chem. B* **2000**, *104*, 9111.
- (6) Mafune, F.; Kohno, J.; Takeda, Y.; Kondow, T. *J. Phys. Chem. B* **2003**, *107*, 4218.
- (7) Sylvestre, J.; Poulin, S.; Kabashin, A.; Sacher, E.; Meunier, M.; Luong, H. *J. Phys. Chem. B* **2004**, *108*, 16864.
- (8) Barcikowski, S.; Hahn, A.; Kabashin, A.; Chichkov, B. *Appl. Phys. A: Mater. Sci. Process.* **2007**, *87*, 47.
- (9) Pyatenko, A.; Shimokawa, K.; Yamaguchi, M.; Nishimura, O.; Suzuki, M. *Appl. Phys. A: Mater. Sci. Process.* **2004**, *79*, 803.
- (10) Kamat, P. V.; Flumiani, M.; Hartland, G. V. *J. Phys. Chem. B* **1998**, *102*, 3123.
- (11) Takami, A.; Kurita, H.; Koda, S. *J. Phys. Chem. B* **1999**, *103*, 1226.
- (12) Link, S.; El-Sayed, M. A. *J. Phys. Chem. B* **1999**, *103*, 4212.
- (13) Link, S.; Burda, C.; Nikoobakh, B.; El-Sayed, M. A. *J. Phys. Chem. B* **2000**, *104*, 6152.
- (14) Smejkal, P.; Pfleger, J.; Siskova, K.; Vickova, B.; Dammer, O.; Slouf, M. *Appl. Phys. A: Mater. Sci. Process.* **2004**, *79*, 1307.
- (15) Ding, L. P.; Fang, Y. *Appl. Surf. Sci.* **2007**, *253*, 4450.
- (16) Pyatenko, A.; Yamaguchi, M.; Suzuki, M. *J. Phys. Chem. B* **2005**, *109*, 21608.
- (17) Pyatenko, A.; Yamaguchi, M.; Suzuki, M. *J. Phys. Chem. C* **2007**, *111*, 7910.
- (18) Yamada, K.; Tokumoto, Y.; Nagata, T.; Mafune, F. *J. Phys. Chem. B* **2006**, *110*, 11751.
- (19) Lugovskoy, A.; Bray, I. *Phys. Rev. B* **1999**, *60*, 3279.
- (20) Davey, W. P. *Phys. Rev.* **1925**, *25*, 753.
- (21) Barnes, S. C.; Singer, K. E. *J. Phys. E: Sci. Instrum.* **1977**, *10*, 737.
- (22) Grua, P.; Moreeuw, J.; Bercegol, H.; Jonusauskas, G.; Vallee, F. *Phys. Rev. B* **2003**, *68*, 035424.
- (23) *Experimental Methods in the Physical Sciences. v.30. Laser Ablation and Desorption*; Miller, D. C., Hanglund, R. F., Jr., Eds.; Academic Press: San Diego, 1998.
- (24) Sonnichsen, C.; Franzl, T.; Wilk, T.; von Plessen, G.; Feldmann, F. *New J. Phys.* **2002**, *4*, 93.
- (25) Anisimov, S.; Kapeliovitch, B.; Perel'man, T. *Zh. Eksp. Teor. Fiz.* **1974**, *66*, 776. Anisimov, S.; Kapeliovitch, B.; Perel'man, T. *Sov. Phys. GETF* **1974**, *39*, 375.
- (26) Link, S.; El-Sayed, M. A. *J. Phys. Chem. B* **1999**, *103*, 8410.
- (27) Groeneveld, R.; Sprik, R.; Lagendijk, A. *Phys. Rev. B* **1992**, *45*, 5079.
- (28) Groeneveld, R.; Sprik, R.; Lagendijk, A. *Phys. Rev. B* **1995**, *51*, 11433.
- (29) Kelly, L.; Jensen, T.; Lazarides, A.; Schatz, G. C. In *Metal Nanoparticles. Synthesis, Characterization and Application*; Feldheim, D. L., Foss, C. A., Jr., Eds.; Dekker: New York, 2002.
- (30) Hodak, J.; Martini, I.; Hartland, G. V. *J. Phys. Chem. B* **1998**, *102*, 6958.
- (31) Jain, P.; Qian, W.; El-Sayed, M. A. *J. Phys. Chem. B* **2006**, *110*, 136.
- (32) Huang, W.; Qian, W.; Prashant, K.; El-Sayed, M. A. *Nano Lett.* **2007**, *7*, 3227.
- (33) *Perry's Chemical Engineers' Handbook*; Green D. W., Perry, R. H., Eds.; McGraw-Hill: New York, 1999.
- (34) Lin, Z.; Zhigilei, L. V. *Phys. Rev. B* **2008**, *77*, 075133.
- (35) Naher, U.; Bjornholm, S.; Frauendorf, S.; Garcias, F.; Guet, C. *Phys. Rep.* **1997**, *285*, 245.
- (36) Saunders, W. A. *Phys. Rev. A* **1992**, *46*, 7028.

JP808300Q